

Self-promotion mechanism for CO electrooxidation on gold†

Paramaconi Rodriguez,^{*a} Nuria Garcia-Araez^{ab} and Marc T. M. Koper^a

Received 14th December 2009, Accepted 23rd April 2010

DOI: 10.1039/b926365a

CO electrooxidation on Au(111), Au(100) and Au(110) electrodes in 0.1 M HClO₄ and 0.1 M NaOH solutions has been studied by means of voltammetric measurements with hanging meniscus rotating bead-type electrodes. It is found that the reaction order in CO concentration is close to unity at potentials close to the onset of CO oxidation, and then it becomes higher than unity at higher potentials for all studied surfaces except for Au(111) in 0.1 M HClO₄. This behavior indicates that CO oxidation on gold takes place through a self-promotion mechanism, in which the presence of CO on the gold surface enhances the adsorption of its own oxidant. Specifically, this mechanism offers a plausible explanation for the higher catalytic activity in alkaline solutions, since CO adsorption is stronger under these conditions, and thus it can lead to a higher enhancement of the adsorption of the oxidant species.

1. Introduction

The present understanding of gold catalysis is still far from complete. Gold was essentially overlooked as catalyst until the late 1980s. Then, since the first report of Haruta,¹ supported gold catalysts have attracted increasing interest because their exceptional catalytic activity toward many important reactions, such as the water–gas shift reaction² and several hydrocarbon oxidations.³ Nevertheless, despite the extensive research in this field, a complete molecular-level insight into the catalytic origin of gold catalysts remains a pending task.

Noteworthy, 24 years before the Haruta's work, the surprising catalytic activity of gold towards the oxidation of CO at room temperature was reported in an electrochemical environment.⁴ One striking aspect of gold electrochemistry, in comparison with gas-phase reactions, is the very important effect of the pH. Alkaline media appear to be optimum for CO electrooxidation on gold, which takes place at *ca.* 0.5 V lower overpotential than in the case of the platinum,⁵ the latter being the most common catalyst in fuel cells.⁶ It is also important to mention that, as opposed to the situation in the gas phase, the electrocatalytic activity of gold also pertains to the bulk material and not just to supported nanoparticles. In addition, gold is used in electrochemical environments to catalyze other important reactions such as hydrocarbon oxidation,^{7,8} borohydride oxidation,⁹ or oxygen reduction,¹⁰ which may have important applications for low-temperature fuel cells.

In order to possibly utilize the unexpected catalytic activity of gold, it is essential to understand the mechanism of gold catalysis. Electrochemical measurements are especially

well-suited to address this task because electrochemistry allows separating the oxidation and reduction reactions. Thus, understanding CO electrooxidation on gold may help to elucidate the gas-phase catalysis on gold. Besides, this approach is also advantageous because CO electrooxidation is catalyzed by gold single-crystal electrodes, and thus this study can be performed under conditions of well-defined electrode structure.

The present work provides a detailed characterization of the kinetics of CO electrooxidation on gold single-crystal electrodes in alkaline and acidic solutions. The experiments were performed by using cyclic voltammetry with hanging meniscus rotating bead-type electrodes. The present work complements a previous study in alkaline media,¹¹ since it extends the characterization of CO electrooxidation to acidic media, and it provides a more detailed analysis of the experimental data. In our previous work,¹¹ we proposed that gold catalysis proceeds through a self-promotion mechanism in which the presence of CO on the electrode surface enhances the adsorption of the oxidant species. The present work provides further experimental support to this model, and also proposes a plausible explanation for the marked pH effect of CO electrooxidation on gold.

2. Materials and methods

The experiments were performed with bead-type gold single-crystal electrodes acquired from icryst. Prior to each experiment the electrodes were annealed in a propane–air flame to red heat and quenched with ultrapure water. A two-compartment electrochemical cell was employed, with a gold wire as the counter electrode and a reversible hydrogen electrode (RHE) as the reference electrode. All potentials in this work are referred to the RHE scale. Electrochemical measurements were performed with an Autolab PGSTAT12. Solutions were prepared from NaOH (99.998%, Sigma-Aldrich) or HClO₄ (Merck, “Suprapur”) and ultra-pure water (MilliQ gradient A10 system, 18.2 MΩ cm). Ar (N66) was used to deoxygenate all solutions and CO (N47, stored in an aluminium cylinder

^a Leiden Institute of Chemistry, Leiden University, PO Box 9502, 2300 RA Leiden, The Netherlands.

E-mail: rodriguezperezpb@chem.leidenuniv.nl;

Fax: +31-71-5274451

^b FOM Institute for Atomic and Molecular Physics (AMOLF), PO Box 41883, 1009 DB Amsterdam, The Netherlands

† Electronic supplementary information (ESI) available: Additional experiments performed with a Teflon-embedded gold polycrystalline rotating disc electrode. See DOI: 10.1039/b926365a

and connected through aluminium valves, in order to prevent iron carbonyl contamination) was used to dose CO.

It should be noted that the contact of the electrode with the electrolyte solution was performed at $E = 0.1$ V, and less than 20 s were required to properly position the electrode in the hanging meniscus configuration. Previous works have shown that the exposure of gold electrodes to CO-containing solutions at low enough potentials leads to the formation of chemisorbed CO species that may inhibit substantially the CO electrooxidation.^{5,12} The formation of such species is negligible under the present experimental conditions, as will be shown in a forthcoming publication.¹³

It should also be mentioned that the voltammetric experiments on CO oxidation on hanging meniscus rotating bead-type single-crystal electrodes were performed with particular caution. The presence of CO in the atmosphere of the electrochemical cell may produce the appearance of an additional oxidation current, whose origin is likely related to the fast diffusion of gas-phase CO to the meniscus solution layer. In order to avoid these complications, previous works embedded the gold electrodes in Teflon.^{14,15} However, that procedure may damage the surface structure of the single-crystal electrodes. For this reason, in the present work, the effect of gas-phase CO has been eliminated by performing the experiments with a blanket of argon. In addition, the flow and duration of the argon flow within the cell atmosphere were minimized, in order to avoid the decrease of the concentration of dissolved CO in solution by argon purging. Furthermore, in order to rule out the possibility that gas-phase CO would interfere in the measurements, additional experiments were performed with a Teflon-embedded polycrystalline gold electrode (see ESI†). In this way, it could be corroborated that the conclusions from this work are not related to an artifact associated to the use of the hanging-meniscus configuration.

3. Results

3.1 Preliminary considerations about the surface structure of Au(111), Au(100) and Au(110) in 0.1 M HClO₄ and 0.1 M NaOH solutions, as a function of potential

Before addressing the analysis of CO electrooxidation on gold single-crystal electrodes, it is first necessary to describe the surface structure of these electrodes and how it changes with potential. Fig. 1 and 2 show the cyclic voltammograms of Au(111), Au(100) and Au(110) electrodes in 0.1 M HClO₄ and 0.1 M NaOH solutions, respectively. The characteristic profiles of the voltammograms in these figures are typical for clean and well-ordered Au(111), Au(100) and Au(110) electrodes, as reported previously in acidic¹⁶ and alkaline¹⁷ media. The surface structure of these electrodes, under electrochemical conditions, has been characterized in several papers by means of *in situ* scanning tunneling microscopy (STM) and X-ray scattering (SXS). It has been shown that the three gold basal planes reconstruct. The Au(100) surface has been studied the most extensively. Several SXS^{18–21} and STM^{22,23} works and electroreflectance measurements²⁴ have shown that Au(100) reconstructs to an incommensurate densely-packed hexagonal layer, with a periodicity close to (5×27) . The

reconstruction is gradually lifted in perchloric acid solutions when the applied potential is higher than *ca.* 0.5 V, leading to the appearance of a small anodic peak at 0.87 V in the cyclic voltammograms recorded at 50 mV s^{-1} .^{18–22,24} After that, the reconstruction is slowly recovered as the potential is decreased below *ca.* 0.3 V for several minutes.^{18–22,24} In alkaline media, the lifting of the reconstruction appears as a sharp anodic peak at 1.0 V in the voltammogram at 50 mV s^{-1} , and after that, the reconstruction is gradually recovered when lower potentials are applied.^{19–21,23,24} It is also worth mentioning that the transition between reconstructed and unreconstructed structures is essentially unaffected by the presence of CO in perchloric acid solutions.^{20,21} In contrast, in CO-saturated alkaline solutions, the lifting of the reconstruction takes place at higher potentials than in CO-free solutions, according to STM and SXS studies.^{21,23} However, as will be shown below, the marked anodic peak characteristic of the lifting of the reconstruction for Au(100) in 0.1 M NaOH (Fig. 2) is also visible in the presence of CO in solution (Fig. 4), and it is observed that its potential is essentially unaffected by the presence of CO.

Several STM^{25,26} and SXS^{27,28} works have shown that the Au(111) surface forms a reconstructed hexagonal ($\sqrt{3} \times 22$) structure at low enough potentials. In 0.1 M HClO₄ solutions, lifting of the reconstruction is induced by application of potentials higher than 0.8 V for 5–10 min.²⁵ The reconstructed surface can be recovered by application of low potentials

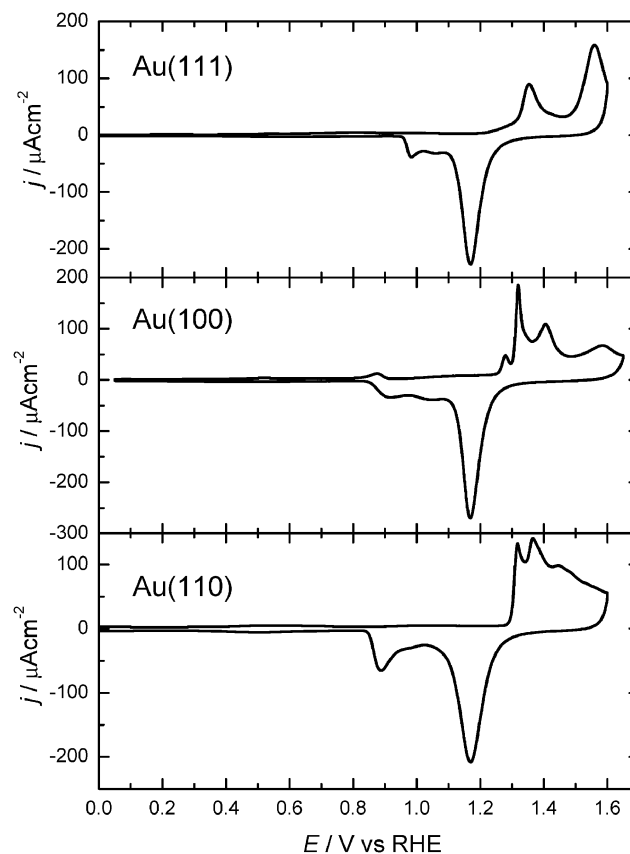


Fig. 1 Cyclic voltammograms of Au(111), Au(100) and Au(110) in 0.1 M HClO₄. Scan rate: 50 mV s^{-1} .

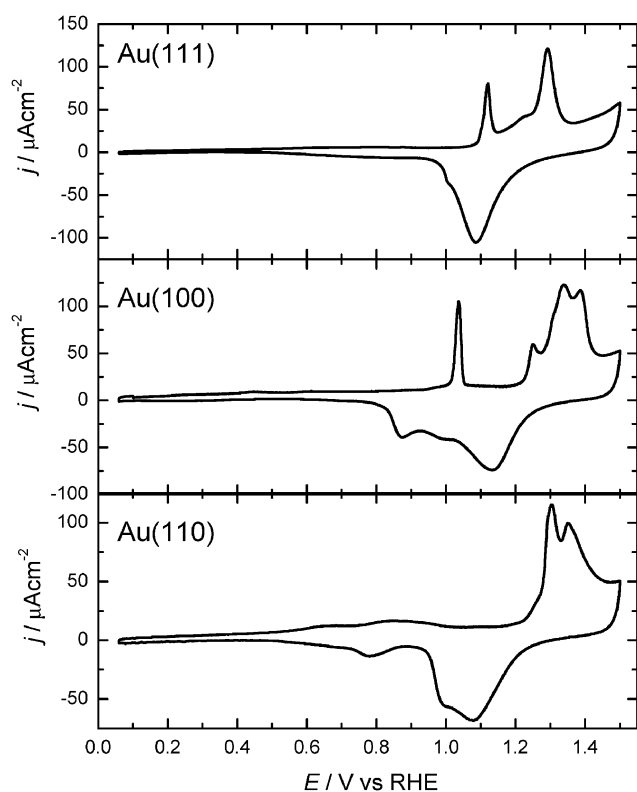


Fig. 2 Cyclic voltammograms of Au(111), Au(100) and Au(110) in 0.1 M NaOH. Scan rate: 50 mV s⁻¹.

(≈ 0 V) for 5–10 min.²⁵ On the other hand, atomic-resolution STM images in CO-saturated 0.1 M HClO₄ solutions show that the transition between the reconstructed and unreconstructed structures takes place between -0.1 and 0.1 V and it is completed in about 10 min.²⁶ On the other hand, in alkaline solutions, the lifting of the reconstruction takes place at *ca.* 1.1 V, concomitant with the sharp voltammetric peak at these potentials, and afterwards, the reconstructed surface is slowly recovered at $E < 0.5$ V.²⁸ In CO-saturated alkaline solutions, the lifting of the reconstruction is shifted *ca.* 0.1–0.2 V towards higher potentials, and its recovery is faster than in the absence of CO.²⁸

Finally, the Au(110) surface in perchloric acid solutions forms, at low potentials, a reconstructed structure with mixed (1 × 2) and (1 × 3) domains.^{29–31} Application of potentials above 0.4–0.5 V induces a fast (nearly immediate) lifting of the reconstruction. Afterwards, the recovery of the reconstructed surface, by application of potentials below 0.0 V, is also very rapid.^{29–31} In alkaline solutions, lifting of the reconstruction takes place at $E > 0.8$ V, and in CO-saturated alkaline solutions, the transition takes place at higher potentials.²⁸

3.2 Bulk CO oxidation on gold single-crystal electrodes under rotating conditions

The bulk CO oxidation was studied by a series of voltammetric measurements with bead-type Au(111), Au(100) and Au(110) electrodes in hanging meniscus rotating disk electrode (HMRDE) configuration, similar to those described in refs. 32 and 33. The use of rotating electrodes allows the characterization

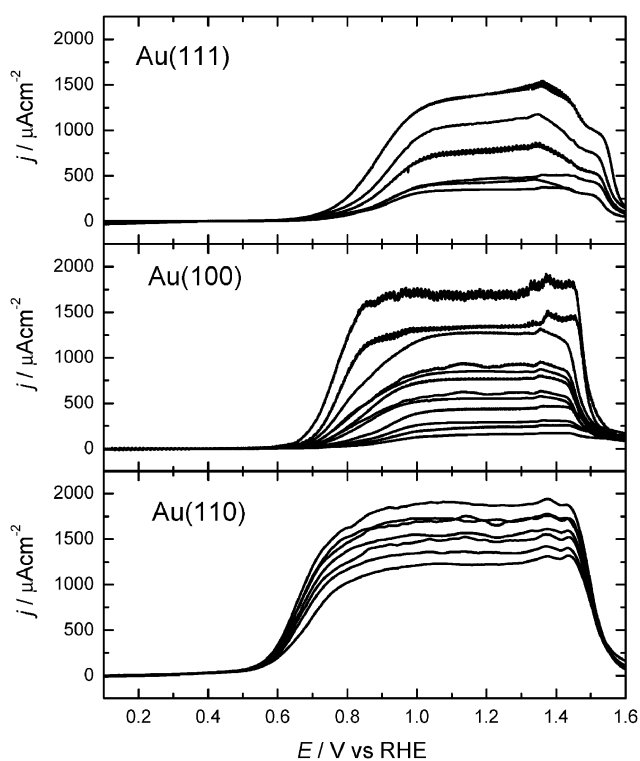


Fig. 3 HMRDE voltammograms of Au(111), Au(110) and Au(100) electrodes in 0.1 M HClO₄ with different CO concentrations. Scan rate: 50 mV s⁻¹. Rotation rate: 1100 rpm.

of the kinetics of bulk CO oxidation under conditions of continuous supply of CO to the electrode surface. This approach is advantageous with respect to the voltammetric measurement under non-rotating conditions, since in the present case, the kinetically-controlled regime extends over a broader potential window, and also, the characterization of the diffusion-limited regime is more straightforward.

We are particularly interested in the characterization of CO oxidation as a function of the CO concentration in solution. In order to vary the CO concentration in solution, the aqueous solutions were purged with a mixture of CO and argon, whose mixing ratio was varied by means of a gas splitter. Fig. 3 and 4 show the HMRDE voltammograms for Au(111), Au(100) and Au(110) in 0.1 M HClO₄ and 0.1 M NaOH, with different CO concentrations at a fixed rotation rate of 1100 rpm. It should be stressed that the electrodes were flame-annealed before each voltammetric measurement, in order to assure that the surface structure is well-ordered.

Fig. 3 and 4 clearly show that CO oxidation on gold is markedly enhanced in alkaline media compared to acid media. In addition, clear differences in the catalytic activity of the three gold basal planes are observed. The present paper is focused on providing a mechanistic understanding of this behavior. We will first discuss the results in acid media. In view of Fig. 3, the bulk CO oxidation in 0.1 M HClO₄ starts at around 0.5 V on Au(111) and Au(100), and at around 0.4 V on Au(110). These potential values agree well with previous reports on non-rotating Au(111),²⁶ Au(100)¹⁴ and Au(110)¹⁴ electrodes. Of course, the shape of the HMRDE voltammograms at higher potentials differs from the results obtained

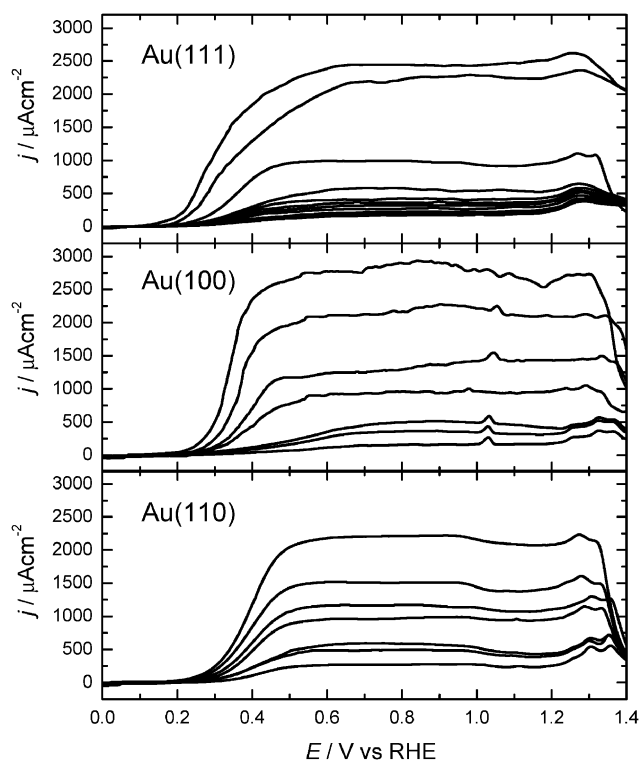


Fig. 4 HMRDE voltammograms of Au(111), Au(110) and Au(100) electrodes in 0.1 M NaOH with different CO concentrations. Scan rate: 50 mV s⁻¹. Rotation rate: 1100 rpm.

under non-rotating conditions. As a result of the depletion of the CO concentration near the electrode, under non-rotating conditions, a maximum CO oxidation current is observed at *ca.* 0.90, 0.75 and 0.65 V on Au(111),²⁶ Au(100)¹⁴ and Au(110)¹⁴ (depending on scan rate). In contrast, much higher CO oxidation currents are achieved when the electrode is rotated at 1100 rpm, as shown in Fig. 3. A mass-transport limited plateau is observed on the HMRDE voltammograms of the three gold basal planes at potentials higher than 1.0 V, reaching a maximum current density of *ca.* 2000 μA cm⁻². Noteworthy, this value of the maximum current density is in reasonable agreement with the theoretical limiting current calculated with the Levich equation:³⁴

$$j_{\text{lim}} = 0.62nFD^{2/3}\nu^{-1/6}c_{\text{CO}}\omega^{1/2} \quad (1)$$

where n is the number of electrons ($n = 2$), F is the Faraday constant ($F = 96485$), D is the diffusion coefficient ($D = 2.0 \times 10^{-5}$ cm² s⁻¹),⁴ ν is the kinematic viscosity ($\nu = 10^{-2}$ cm² s⁻¹ in pure water),³⁵ c_{CO} is the bulk CO concentration ($c_{\text{CO}} = 1.06$ mM in CO-saturated pure water at 1 atm),³⁵ and ω is the angular rotation rate ($\omega = 1100$ rpm = 115.2 rad s⁻¹). Putting these numbers together gives $j_{\text{lim}} \approx 2200$ μA cm⁻², in reasonable agreement with the experimental value.

Next, we will discuss the bulk CO oxidation in alkaline media. Fig. 4 shows that the onset of CO oxidation on gold in 0.1 M NaOH takes place at around 0.1 V on Au(111) and Au(100) and at around 0.2 V on Au(110). These onset potential values are about 0.5 V lower than in acid media. Similar differences in the catalysis of polycrystalline gold electrodes in acid and alkaline solutions were reported by Kita *et al.*⁵

(a decrease of the onset of the bulk CO oxidation by 0.5 V was observed in 1 M NaOH with respect to 1 M HClO₄). Besides, the catalysis of gold on CO oxidation in alkaline media is so active, that at potentials above 0.40 V, the mass transport limited current is achieved for the three basal planes. This maximum current density equals *ca.* 2500 μA cm⁻², which is somewhat higher than in acid media. This is probably due to the fact that the maximum CO concentration achieved in the present experiments in alkaline media reached the saturation value, while in acidic media the maximum CO concentration was lower than saturation. This may be related to the fact that saturation with CO of perchloric acid solutions required much longer purging times than in alkaline solutions.

Finally, it should be noted that the present results are not in agreement with previous reports¹⁵ on the bulk CO electro-oxidation on RDE Au(111), Au(100) and Au(110) electrodes in 0.1 M HClO₄ and 0.1 M KOH. Only in the case of Au(111) and Au(100) in 0.1 M HClO₄ solutions the RDE voltammograms are in reasonable agreement with the present work. In all other cases, the onset of CO electrooxidation takes place at clearly higher potentials (the onset potential values being between 0.1–0.3 V higher than in the present work). In this regard, it should be noted that the blank voltammograms in this work show a much higher degree of surface order and absence of surface impurities than those in ref. 15. This is probably related to the fact that the present work was performed with bead-type electrodes under meniscus configurations, while in ref. 15 the electrode was embedded in Teflon.

3.3 Apparent transfer coefficient

The onset of the bulk CO oxidation is kinetically controlled. The measured current density is independent of the potential scan rate and the rotation rate of the electrode. Besides, the transitions between the reconstructed and unreconstructed surfaces most likely take place at potentials outside this potential region (see section 3.1). Consequently, within this region, the apparent transfer coefficient, α , can be determined from the fit of the logarithm of the current density *vs.* potential. The results of these fits at selected CO concentrations are shown in Fig. 5 and 6. In perchloric acid solutions, $\alpha = 0.4$ –0.3 for Au(111), $\alpha = 0.6$ –0.4 for Au(100) and $\alpha = 0.5$ –0.4 for Au(110). In sodium hydroxide solutions, $\alpha = 0.6$ –0.4 for Au(111), $\alpha = 0.6$ –0.3 for Au(100) and $\alpha = 0.5$ for Au(110). In all cases, higher α values correspond to higher CO concentrations in solution.

Previous kinetic studies of 0.1 M HClO₄ solutions reported $\alpha = 0.53$ for Au(111), $\alpha = 0.55$ for Au(100)-hex and $\alpha = 0.73$ for Au(110).^{23,36} Although the present results for Au(111) and Au(100) are in reasonable agreement with these values, the value of α for Au(110) obtained here is clearly smaller. In order to explain these differences, we performed additional experiments with an Au(110) electrode whose surface structure had been distorted by successive cycling between 0 and 1.6 V, leading to $\alpha = 0.6$. In addition, if the value of α is evaluated from the values of the potential at the current peak and at one-half and one-quarter of the peak current, following ref. 36, a value of α in much closer agreement with the value reported in ref. 23 and 36 ($\alpha = 0.73$) is obtained ($\alpha = 0.7$). Therefore, the

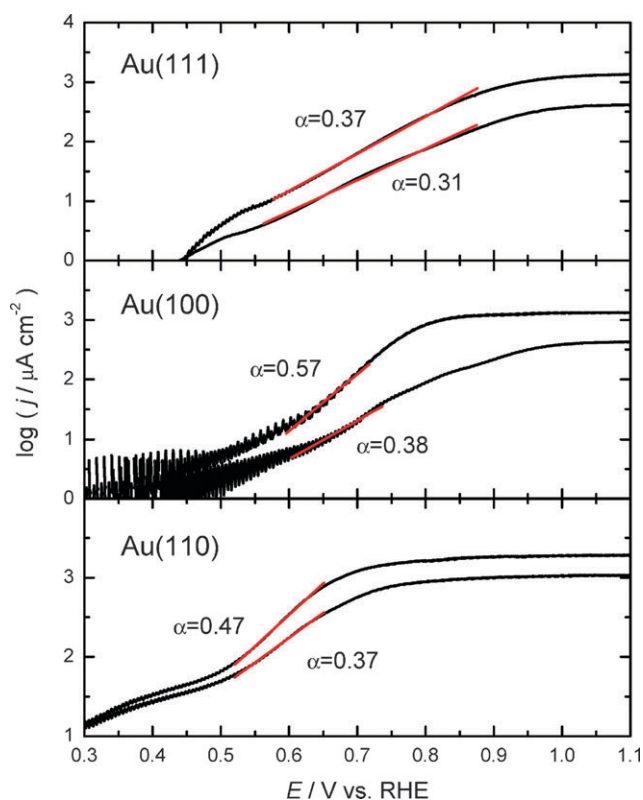


Fig. 5 Plot of the logarithm of the current density vs. potential, as obtained from the experimental data for CO oxidation in 0.1 M HClO₄ in Fig. 3. The linear fits within the kinetically-controlled regime and the corresponding α values are also shown.

differences with previous works mainly originate from the different methods of evaluation of α and the different degree of surface order.

Finally, it is worth mentioning that for CO oxidation on polycrystalline gold in 1 M NaOH, previous works reported that $\alpha = 0.49$ ³⁷ and $\alpha = 0.50$.⁴ These results are in excellent agreement with the present value ($\alpha = 0.5$) for Au(110) in 0.1 M NaOH.

3.4 Reaction order in CO concentration

The experimental data in Fig. 3 and 4 can be used to evaluate the reaction order in CO concentration for the CO electro-oxidation on gold, as previously explained.¹¹ This is done by plotting the logarithm of the current at a selected potential where the reaction is kinetically controlled, vs. the logarithm of the current at a higher potential where the reaction is diffusion limited. This analysis takes advantage of the fact that the diffusion-limited current will be proportional to the CO concentration in solution, c_{CO} , while the kinetically-limited current will be proportional to c_{CO}^r , where r is the reaction order. Fig. 7 and 8 show the results of this analysis in acid and alkaline media, respectively. The diffusion limited current has been evaluated at $E = 1.2$ V in perchloric acid solutions and at $E = 0.8$ V in sodium hydroxide solutions, but essentially the same results are obtained by using the measured current at other potentials within the mass-transport controlled plateau. The kinetically limited current is evaluated at

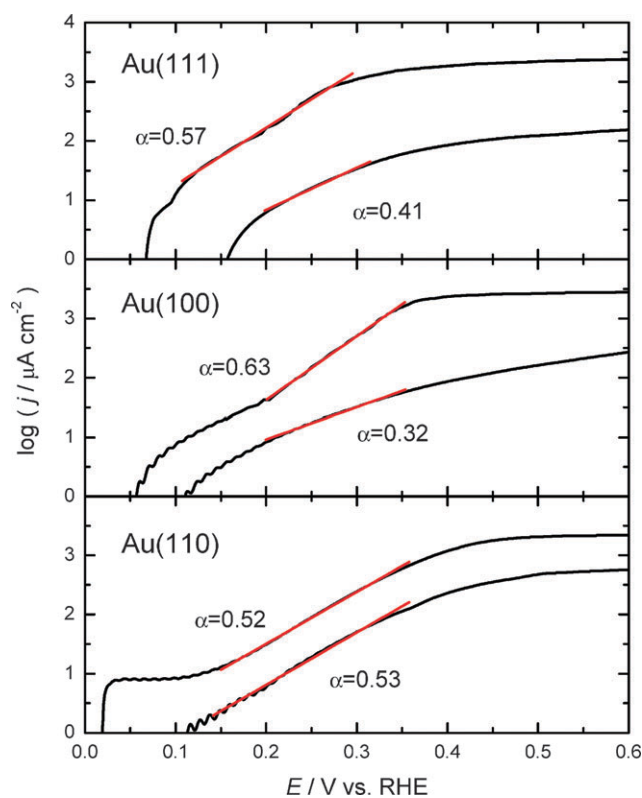


Fig. 6 Plot of the logarithm of the current density vs. potential, as obtained from the experimental data for CO oxidation in 0.1 M NaOH in Fig. 4. The linear fits within the kinetically-controlled regime and the corresponding α values are also shown.

different potentials within the rising branch of the bulk CO oxidation curve, within the potential window used in the evaluation of the effective charge transfer coefficients in section 3.3.

The values of the slope of the plots in Fig. 7 and 8 equal the value of the reaction order, r . It is observed that at potentials close to the onset of CO oxidation, $r \approx 1$. Then, at higher potentials, values of $r > 1$ are measured in all cases except for Au(111) in 0.1 M HClO₄. Noteworthy, values of the reaction order in CO concentration higher than unity have also been reported by Kita *et al.*⁵ for CO oxidation on polycrystalline gold in 1 M NaOH ($r = 1.15$). Conversely, Weaver and co-workers¹⁴ reported a reaction order of $r = 1.0 \pm 0.1$ on Au(110) in both acid and alkaline media, within the whole potential window for the CO oxidation. The discrepancy of this latter result originates from the fact that, in the work of Weaver *et al.*, values of the reaction order were estimated indirectly from the analysis of non-rotating voltammetric data. This evaluation involves a complex mathematical analysis, which *a priori* assumes $r \equiv 1$. On the contrary, the present evaluation employs the pure experimental data, and thus provides a more accurate and reliable evaluation of reaction orders.

In order to double-check the present findings, additional experiments were performed with a Teflon-embedded gold polycrystalline electrode (see ESI†). These experiments were performed with the electrode completely submerged in the electrolyte solution, and thus any possible interference from

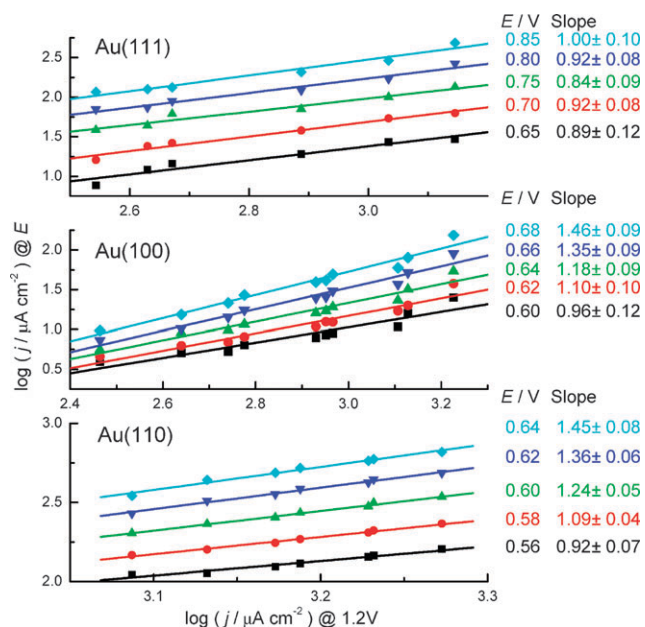


Fig. 7 Plot of the logarithm of the kinetically limited current at selected potentials, as indicated, vs. the logarithm of the mass-transport limited current at $E = 1.2$ V, as obtained from experimental data for CO oxidation in 0.1 M HClO₄ in Fig. 3.

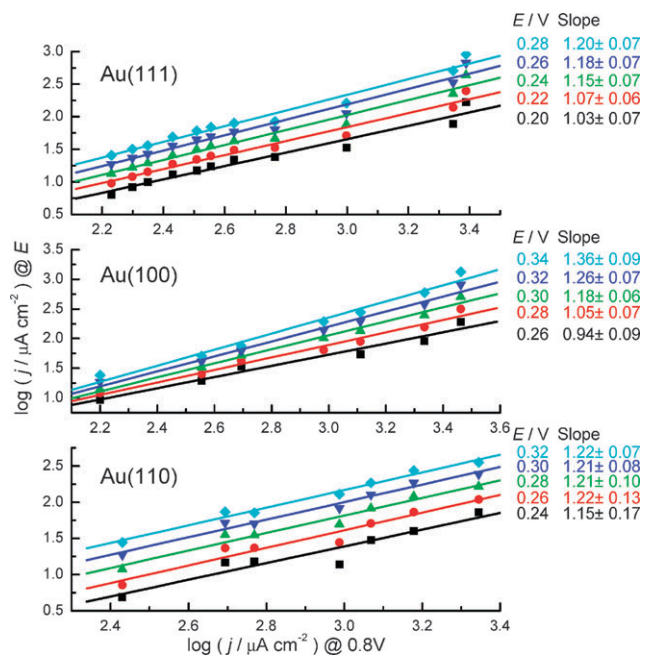
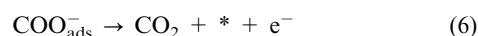
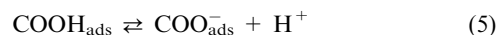


Fig. 8 Plot of the logarithm of the kinetically limited current at selected potentials, as indicated, vs. the logarithm of the mass-transport limited current at $E = 0.8$ V, as obtained from experimental data for CO oxidation in 0.1 M NaOH in Fig. 4.

gas-phase CO is fully eliminated. It was found that the electrooxidation of CO on polycrystalline gold exhibits essentially the same behavior as Au(110). Furthermore, values of the reaction order in CO concentration $r \approx 1$ have been obtained at the beginning of the CO electrooxidation, and then, at higher potentials, $r > 1$.

4. Discussion

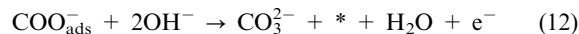
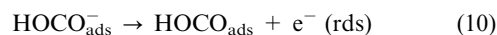
We have recently proposed a new interpretation of the mechanism for CO oxidation of gold.¹¹ According to this mechanism, CO promotes its own oxidation *via* the enhancement of the adsorption of its own oxidant (most probably, OH⁻ species). The mechanism is based on a DFT calculation that shows that OH and CO enhance each other's adsorption when bonded to nearest-neighbor (nn) binding sites on the gold surface. From this, the following mechanism can be proposed in alkaline media:



where rds stands for rate-determining step. The CO₂ formed would quickly form carbonate in alkaline media. In acidic media, reaction (3) would be replaced by:

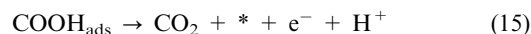
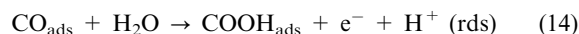


The mechanism proposed here is similar to that proposed by Roberts⁴ and Kita⁵ for CO electrooxidation in alkaline media. The main difference is that they considered the formation of the reactant-pair HOCO_{ads}⁻, according to:



However, the formation of the reactant-pair HOCO_{ads}⁻ has not been confirmed by spectroscopic studies. On the contrary, adsorbed CO species on gold have been clearly identified by a number of spectroscopic studies,^{12,38–42} thus supporting the mechanism proposed here.

On the other hand, Weaver *et al.*¹⁴ proposed the following mechanism in acidic media:



However, this mechanism is not in agreement with the experimental value of the reaction order in H⁺ concentration of -1 .

The mechanism proposed here considers that the oxidant species for CO electrooxidation are anionic OH⁻ species adsorbed on nearest-neighbor sites. As a result, the reaction order in OH⁻ and H⁺ concentrations would be 1 and -1 , in alkaline and acidic media, respectively, in agreement with the experiments.^{4,5,14} In this regard, thermodynamic studies⁴³ have shown that the polarity of the Au(111)–OH bond is large at the onset of OH⁻ adsorption, suggesting that the adsorbed

species can be considered anionic. Moreover, in the simplest case in which the rate-determining electron-transfer reaction has a symmetrical barrier, the above mechanism predicts a transfer coefficient close to $\alpha = 0.50$, which is in agreement with the experimental results on polycrystalline gold ($\alpha = 0.49$,⁵ $\alpha = 0.50$ ⁴) and with the present results for gold single-crystal electrodes.

If there were no dependence of the adsorption energies of the various species on the potential, then the above mechanism would predict very similar kinetics in alkaline and acidic media, on the RHE scale. However, there is strong evidence for the enhanced binding of CO_{ads} on gold in alkaline media (see discussion below), and we suggest that this causes the enhanced reaction kinetics in alkaline media.

At steady state, the CO₂ production current is given by:

$$j = 2Fk\theta_{\text{CO}}\theta_{\text{Ox}} \quad (16)$$

where 2 is the number of electrons transferred when the CO is oxidized to CO₂, F the Faraday constant, k the oxidation rate constant, θ_{CO} the CO coverage and θ_{Ox} is the coverage of the oxidant species on the surface (most likely, θ_{OH^-}). If the adsorption energy of the oxidant species is enhanced by the presence of CO on the surface through a linear dependence on the CO coverage, one could write for θ_{Ox} :

$$\theta_{\text{Ox}} = \theta_{\text{Ox}}^0 \exp(\gamma\theta_{\text{CO}}) \quad (17)$$

From this simple assumption, it follows that the reaction order, r , in CO concentration, c_{CO} , will be given by:¹¹

$$r = \frac{d \ln j}{d \ln c_{\text{CO}}} = 1 + \gamma\theta_{\text{CO}} \quad (18)$$

Hence this model predicts a reaction order in c_{CO} of $r > 1$ if $\gamma > 0$. In conclusion, the self-promotion mechanism is able to explain the present experimental results of reaction orders in c_{CO} higher than unity, for Au(111), Au(100) and Au(110) in acid and alkaline solutions.

Furthermore, the self-promotion mechanism also offers a plausible explanation for the marked pH-effect on gold catalysis for CO oxidation. DFT calculations¹¹ have shown that the CO and OH enhance each other's binding, through a local gold-mediated donation-back donation mechanism driven by a change in the local electrostatics. Consequently, the enhancement of the adsorption of oxidative species by CO adsorption will critically depend on the CO adsorption energy itself. A higher interaction of CO species with the gold surface will allow for a higher stabilization of co-adsorbed oxidative species. In turn, the consequent increase of the coverage of oxidative species will lead to further strengthening of CO adsorption. Therefore, the enhanced catalytic activity of gold electrodes in alkaline solutions may be explained by the higher adsorption energy of CO species under these conditions.

Several works have shown that irreversible adsorption of CO takes place on gold electrodes in alkaline solutions.^{5,42} Conversely, in acid media, CO does not remain chemisorbed on the gold surface in the absence of CO in solution.^{26,39,41} This behavior is understandable from the point of view that in alkaline media, CO adsorption is studied at more negative potentials (*vs.* SHE) than in acidic media, even if the CV is plotted on the reversible hydrogen electrode scale (RHE). At

more negative potentials (*vs.* SHE), more electronic surface states become filled, and thus they can contribute to the formation of the Au–CO bond. Indeed, electroreflectance measurements⁴⁴ showed that strong CO chemisorption on gold only takes place at potentials below a threshold only achievable in alkaline media, and was accompanied by a significant change in the electroreflectance due to the filling of certain surface states.

Conclusions

Here we have reported a new interpretation of the kinetics of CO oxidation on Au(111), Au(100) and Au(110) electrodes in 0.1 M HClO₄ and 0.1 M NaOH solutions. We have performed voltammetric experiments with hanging meniscus rotating bead-type electrodes as a function of the CO concentration in solution. It has been shown that the apparent transfer coefficient for CO electrooxidation is $\alpha = 0.4$ – 0.3 for Au(111), $\alpha = 0.6$ – 0.4 for Au(100) and $\alpha = 0.5$ – 0.4 for Au(110) in 0.1 M HClO₄, and $\alpha = 0.6$ – 0.3 for Au(100) and $\alpha = 0.5$ for Au(110) in 0.1 M NaOH. These values are in reasonable agreement with previous studies,^{23,36} and indicate that the rate-determining step is a first-electron transfer step, as previously proposed.^{4,37} Furthermore, the present experimental data show that the reaction order in CO concentration is $r \approx 1$ at the beginning of the CO oxidation, but $r > 1$ at higher potentials (except for Au(111) in 0.1 M HClO₄). This agrees with a mechanism in which CO electrooxidation proceeds through a self-promotion mechanism, whereby CO adsorption enhances the adsorption of its own oxidant species. This may explain the higher catalytic activity in alkaline solutions, since the affinity of CO to gold electrodes is known to increase at higher pH, leading to a stronger enhancement of the adsorption of the oxidant species.

Acknowledgements

The authors acknowledge financial support from the Netherlands Organization for Scientific Research (NWO), the European Commission (through FP7 Initial Training Network “ELCAT”, Grant Agreement No. 214936-2). NG acknowledges the European Commission (FP7) for the award of a Marie Curie fellowship

References

- 1 M. Haruta, N. Yamada, T. Kobayashi and S. Ijima, *J. Catal.*, 1989, **115**, 301.
- 2 Q. Fu, H. Saltsburg and M. Flytzani-Stephanopoulos, *Science*, 2003, **301**, 935–938.
- 3 M. D. Hughes, Y.-J. Xu, P. Jenkins, P. McMorn, P. Landon, D. I. Enache, A. F. Carley, G. A. Attard, G. J. Hutchings, F. King, E. H. Stitt, P. Johnston, K. Griffin and C. J. Kiely, *Nature*, 2005, **437**, 1132–1135.
- 4 J. L. Roberts and D. T. Sawyer, *Electrochim. Acta*, 1965, **10**, 989–1000.
- 5 H. Kita, H. Nakajima and H. Kimitaka, *J. Electroanal. Chem. Interfacial Electrochem.*, 1985, **190**, 141–156.
- 6 *Fuel Cell Catalysis: A Surface Science Approach*, ed. M. T. M. Koper, John Wiley and Sons, Inc, Hoboken New Jersey, USA, 2009.
- 7 S.-C. Chang, Y. Ho and M. J. Weaver, *J. Am. Chem. Soc.*, 1991, **113**, 9506–9513.

- 8 J. Hernandez, J. Solla-Gullon, E. Herrero, A. Aldaz and J. M. Feliu, *Electrochim. Acta*, 2006, **52**, 1662–1669.
- 9 F. A. Coowar, G. Vitins, G. O. Mepsted, S. C. Waring and J. A. Horsfall, *J. Power Sources*, 2008, **175**, 317–324.
- 10 J. Hernandez, J. Solla-Gullon, E. Herrero, A. Aldaz and J. M. Feliu, *J. Phys. Chem. C*, 2007, **111**, 14078–14083.
- 11 P. Rodriguez, A. A. Koverga and M. T. M. Koper, *Angew. Chem.*, 2010, **122**, 1263–1265.
- 12 S.-C. Chang, A. Hamelin and M. J. Weaver, *Surf. Sci.*, 1990, **239**, L543–L547.
- 13 P. Rodriguez, N. Garcia-Araez, A. A. Koverga, S. Frank and M. T. M. Koper, *Langmuir*, 2010, DOI: 10.1021/la902251z.
- 14 G. J. Edens, A. Hamelin and M. J. Weaver, *J. Phys. Chem.*, 1996, **100**, 2322–2329.
- 15 B. B. Blizanac, M. Arenz, P. N. Ross and N. M. Markovic, *J. Am. Chem. Soc.*, 2004, **126**, 10130–10141.
- 16 A. Hamelin, *J. Electroanal. Chem.*, 1996, **407**, 1–11.
- 17 A. Hamelin, M. J. Sottomayor, F. Silva, S.-C. Chang and M. J. Weaver, *J. Electroanal. Chem. Interfacial Electrochem.*, 1990, **295**, 291–300.
- 18 B. M. Ocko and J. Wang, *Phys. Rev. Lett.*, 1990, **65**, 1466–1469.
- 19 I. M. Tidswell, N. M. Markovic, C. A. Lucas and P. N. Ross, *Phys. Rev. B: Condens. Matter*, 1993, **47**, 16542–16553.
- 20 R. R. Adzic, J. X. Wang, O. M. Magnussen and B. M. Ocko, *Langmuir*, 1996, **12**, 513–517.
- 21 B. B. Blizanac, C. A. Lucas, M. E. Gallagher, M. Arenz, P. N. Ross and N. M. Markovic, *J. Phys. Chem. B*, 2004, **108**, 625–634.
- 22 X. Gao, A. Hamelin and M. J. Weaver, *Phys. Rev. B: Condens. Matter*, 1992, **46**, 7096–7102.
- 23 G. J. Edens, X. Gao, M. J. Weaver, N. M. Markovic and P. N. Ross, *Surf. Sci.*, 1994, **302**, L275–L282.
- 24 D. M. Kolb and J. Schneider, *Electrochim. Acta*, 1986, **31**, 929–936.
- 25 X. Gao, A. Hamelin and M. J. Weaver, *J. Chem. Phys.*, 1991, **95**, 6993–6996.
- 26 C.-H. Shue, L.-Y. O. Yang, S.-L. Yau and K. Itaya, *Langmuir*, 2005, **21**, 1942–1948.
- 27 J. Wang, B. M. Ocko, A. J. Davenport and H. S. Isaacs, *Phys. Rev. B: Condens. Matter*, 1992, **46**, 10321–10338.
- 28 M. E. Gallagher, B. B. Blizanac, C. A. Lucas, P. N. Ross and N. M. Markovic, *Surf. Sci.*, 2005, **582**, 215–226.
- 29 X. Gao, G. J. Edens, A. Hamelin and M. J. Weaver, *Surf. Sci.*, 1994, **318**, 1–20.
- 30 X. Gao, A. Hamelin and M. J. Weaver, *Phys. Rev. B: Condens. Matter*, 1991, **44**, 10983–10986.
- 31 O. M. Magnussen, J. Wiechers and R. J. Behm, *Surf. Sci.*, 1993, **289**, 139–151.
- 32 B. D. Cahan and H. M. Villullas, *J. Electroanal. Chem. Interfacial Electrochem.*, 1991, **307**, 263–268.
- 33 M. D. Macia, J. M. Campiña, E. Herrero and J. M. Feliu, *J. Electroanal. Chem.*, 2004, **564**, 141–150.
- 34 For hanging meniscus rotating electrodes, a correction term should be included in the Levich equation in order to properly describe the hydrodynamics in the meniscus configuration.³² However, previous work has shown that this correction is unnecessary for experiments performed with small bead-type electrodes, as those used here³³.
- 35 *Handbook of Chemistry and Physics*, CRC Press, Boca Raton, FL, 2004.
- 36 S.-C. Chang, A. Hamelin and M. J. Weaver, *J. Phys. Chem.*, 1991, **95**, 5560.
- 37 H. Kita, H. Naohara, T. Nakato, S. Taguchi and A. Aramata, *J. Electroanal. Chem.*, 1995, **386**, 197–206.
- 38 K. Kunimatsu, A. Aramata, H. Nakajima and H. Kita, *J. Electroanal. Chem. Interfacial Electrochem.*, 1986, **207**, 293–307.
- 39 S.-G. Sun, W.-B. Cai, L.-J. Wan and M. Osawa, *J. Phys. Chem. B*, 1999, **103**, 2460–2466.
- 40 G. L. Beltramo, T. E. Shubina and M. T. M. Koper, *Chem-PhysChem*, 2005, **6**, 2597–2606.
- 41 S. Pronkin, M. Hara and T. Wandlowski, *Russ. J. Electrochem.*, 2006, **42**, 1177–1192.
- 42 P. Rodriguez, J. M. Feliu and M. T. M. Koper, *Electrochem. Commun.*, 2009, **11**, 1105–1108.
- 43 A. C. Chen and J. Lipkowsky, *J. Phys. Chem. B*, 1999, **103**, 682–691.
- 44 A. Cuesta, N. Lopez and C. Gutierrez, *Electrochim. Acta*, 2003, **48**, 2949–2956.